

DOE/NASA/20320-64  
NASA TM-86986

(NASA-TM-86986) EFFECT OF PRECIPITATION ON  
WIND TURBINE PERFORMANCE Final Report  
(NASA) 23 p HC A02/MF A01 CSCL 10A

N85-27385

Unclas  
G3/44 21329

# Effect of Precipitation on Wind Turbine Performance

Robert D. Corrigan  
National Aeronautics and Space Administration  
Lewis Research Center

and

Richard D. DeMiglio  
Sverdrup, Inc.

May 1985



Prepared for  
**U.S. DEPARTMENT OF ENERGY**  
**Conservation and Renewable Energy**  
**Wind Energy Technology Division**

DOE/NASA/20320-64  
NASA TM-86986

## **Effect of Precipitation on Wind Turbine Performance**

Robert D. Corrigan  
National Aeronautics and Space Administration  
Lewis Research Center  
Cleveland, Ohio 44135

and

Richard D. DeMiglio  
Sverdrup, Inc.  
Middleburg Heights, Ohio 44130

May 1985

Work performed for  
U.S. DEPARTMENT OF ENERGY  
Conservation and Renewable Energy  
Wind Energy Technology Division  
Washington, D.C. 20545  
Under Interagency Agreement DE-AI01-76ET20320

## EFFECT OF PRECIPITATION ON WIND TURBINE PERFORMANCE

Robert D. Corrigan  
National Aeronautics and Space Administration  
Lewis Research Center  
Cleveland, Ohio 44135

and

Richard D. DeMiglio  
Sverdrup, Inc.  
Middleburg Heights, Ohio 44130

### SUMMARY

During performance testing on the NASA/DOE Mod-0 100 kW wind turbine, a decrease in rotor power was noted during adverse weather conditions (rain, snow, etc.). A review of the test results indicated this decrease could be attributed to the effects of precipitation on the rotor. Because the decrease in performance was significant, additional tests were run to measure and compare the rotor power with and without precipitation. This report presents both the experimental and analytical analysis of the effects of precipitation on wind turbine performance.

The tests were conducted on the two-bladed Mod-0 horizontal-axis wind turbine with three different rotor configurations. Experimental data from these tests are presented which indicate that rainfall degraded the performance of all three rotors. Light rainfall degraded performance by as much as 20 percent at higher windspeeds while heavy rainfall degraded performance by as much as 30 percent. Snow mixed with drizzle degraded performance by as much as 36 percent at low windspeeds.

The theoretical analysis which was used to predict the effect of rain on wind turbine performance was based on a blade-element/momentum code with airfoil characteristics modified to account for the effect of rain. The predictions were made for one of the three rotor configurations tested and indicated a loss in performance of 31 percent at high windspeeds with moderate rainfall rates. These predicted results agreed well with experimental data.

### INTRODUCTION

Wind turbines operate in the open environment, hence they are exposed to various weather conditions (rain, snow, etc.). Recent tests at the Mod-0 wind turbine site have indicated that the performance of the machine, measured as power output as a function of windspeed, decreased during rainy weather conditions as compared to operation without rain. This phenomenon, if characteristic of all types of wind turbines, may have a significant effect on economics, especially when turbines are located in predominantly rainy environments.

In view of the previous observations, a research effort was conducted to study the effects of precipitation on wind turbine performance. Specific objectives of this effort were: (1) to quantify the effects of precipitation on the Mod-0 wind turbine configured with three different rotors as a means of evaluating the generality of the phenomenon, and (2) to present and evaluate a method for adjusting airfoil characteristics to rain effects to provide data that can be used as input for a rotor-performance prediction model. The method for modifying the airfoil characteristics was developed by J. Luers and P. Haines at the University of Dayton Research Institute (refs. 1 to 3).

This report compares the measured performance of three different wind turbine rotor configurations operated during rainy and dry weather conditions in order to provide data about the effects of rain on wind turbine performance. Additionally, the effects of rain on wind turbine rotor performance were predicted for one rotor configuration using a blade-element/momentum code with input airfoil characteristics modified to reflect the effects of rain. Finally, a comparison was then made between the predicted and the actual rotor performance. This comparison was made in order to evaluate the application of the method of correcting airfoil characteristics for rain effects in a rotor-performance prediction code.

### Effects of Rain

Rainfall has three distinct effects on the performance of a moving airfoil. One effect is a loss in the momentum of the moving airfoil as a result of the mass of raindrops adhering to the airfoil surface which must be accelerated to the speed of the airfoil. A second effect is the additional weight of the water adhering to the airfoil surface. The third effect is the change in the condition of the airfoil surface as a result of the adherence and impact of raindrops.

A preliminary analysis was made of the importance of each of these three effects on wind turbine rotor performance. Loss in wind turbine rotor momentum was determined to be ~1 kW for a 38-m-diameter rotor operating at 20 rpm in a rainfall rate of 50 mm/hr. The additional weight of the adhering water had no effect on a wind turbine with more than one rotor because the resulting torques on the blades balanced out at the rotor shaft. The third effect, change of the airfoil surface characteristics, caused rain-induced roughness and appeared to have the most significant impact on wind turbine applications. This rain-induced roughness originates from three sources: (1) waves that develop in the water-film layer on the airfoil surface, (2) water globules that dot the blade surface when there is insufficient rain to form a water film, and (3) disturbances in the water-film layer from the impact of raindrops (ref. 1).

### SYMBOLS

$C_D$	drag coefficient
$C_{D,0}$	drag coefficient at zero angle of attack
$C_L$	lift coefficient

$C_{L,max}$	maximum lift coefficient
$K_s$	equivalent sand grain height, mm
$L$	chord length, m
$P_1$	rotor power, kW
$P_j$	rotor power adjusted to sea-level standard conditions, kW
$P_3$	alternator power, kW
$p_L$	local barometric pressure, mm Hg
$p_0$	standard sea-level barometric pressure, mm Hg
$T_L$	local air temperature, K
$T_0$	standard sea-level temperature, K
$\Delta( )$	difference in a given parameter
$\alpha$	angle of attack, deg
$\alpha_{stall}$	stall angle of attack, deg
$\delta$	control deflection angle, deg

## TEST CONFIGURATIONS AND PROCEDURES

The test data presented in this report were taken at the DOE/NASA Mod-0 Horizontal-Axis Wind Turbine Facility in Sandusky, Ohio. The Mod-0 wind turbine (fig. 1) consists of a rotor/nacelle assembly mounted atop a tubular tower with the rotor axis 38 m above the ground. The rotor performance data presented show the effects of rain collected on three rotor configurations, each differing in their tip sections and operating conditions. All three rotors were two-bladed, coned 3°, and allowed to teeter  $\pm 6^\circ$ .

### Rotor Configurations

The three rotors tested are shown in figures 2 to 4. Rotor configuration I was a tip-controlled rotor with a 12.5-percent span pitchable tip section. The blade (fig. 2) was 15.3 m long, tapered, untwisted, and mounted with a pitch angle of 0° relative to the plane of rotation. It consisted of two sections; a 12.22-m inboard section and a 3.08-m transition/tip-control section. The inner section of the blade was constructed of laminated wood and covered with a polyurethane paint. It had a truncated chord over the inner 4 m. The outer section of the blade utilized a NACA 23024 airfoil section and had smooth and rigid surfaces. The transition/tip-control section was constructed of sheet metal over ribs and covered with a polyurethane paint. It also utilized a NACA 23024 airfoil section and had smooth and rigid surfaces. For these tests the tip section was set to a pitch angle of 0°.

Rotor configuration II was an aileron-controlled rotor with 20-percent chord ailerons. The blade (fig. 3) was 19.5 m long, tapered, untwisted, and mounted with a pitch angle of  $0^\circ$  relative to the plane of rotation. It also consisted of two sections; a 12.22-m section and a 7.88-m aileron-tip section. The inner section is identical to that of configuration I and mounted with a  $0^\circ$  pitch angle relative to the plane of rotation. The aileron-tip section was constructed of fiberglass cloth over foam and covered with a polyurethane paint. The ailerons spanned the outer 30 percent of the blade and were deflected at  $+8^\circ$  (aileron trailing edge toward high-pressure side of airfoil). The aileron-tip section utilized a NACA 23024 airfoil section and had smooth and rigid surfaces.

Rotor configuration III was an aileron-controlled rotor utilizing 38-percent chord ailerons. The blade (fig. 4) was 19.5 m long with twisted and varied airfoil sections. It also consisted of a 12.22-m inboard section and a 7.28-m aileron-tip section. The inboard section was identical to that of configurations I and II where the blade was mounted with a  $0^\circ$  pitch angle relative to the plane of rotation. The aileron-tip section was constructed of sheet metal over ribs and covered with a polyurethane paint. These provided smooth and rigid surfaces. This section of the blade utilized NACA 64 series airfoils and was twisted. The blade twist was as follows: NACA 64-624 with a  $3^\circ$  twist at station 13.09 ranging to a NACA 64-615 with a  $1^\circ$  twist at station 19.20. As specified in the plan for a previous test, the leading edge of this section had a trip strip to cause early transition in the boundary layer from laminar to turbulent. This trip strip remained on the section during testing of precipitation effects. The ailerons spanned the outer 30 percent of the blade and were set to a deflection angle of  $0^\circ$ . A short transition section was utilized to smoothly change from the NACA 23024 to the NACA 64-624 airfoil.

### Operating Conditions

The test data reported in this document were obtained on the Mod-0 wind turbine with the rotor operating downwind of the tower and in controlled yaw. For all rotor configurations, yaw alignment of the wind turbine was maintained to within  $\pm 5^\circ$  of the wind direction. Rotor configuration I was operated at a nominal 31 rpm rotor speed. Rotor configurations II and III were operated at a nominal 20 rpm rotor speed. In all configurations the control surfaces were fixed in position during these tests: the configuration I tip was set at  $0^\circ$ , the configuration II aileron was set at  $+8^\circ$ , and the configuration III ailerons were set at  $0^\circ$ .

### Test Measurements

Wind turbine operating data were taken from sensors mounted on the wind turbine or in the control room. These data included alternator power, rotor speed, and yaw angle. Wind data were taken from instruments mounted at the rotor hub height on an array of five measuring station towers, each located 59.4 m (1.5 rotor diameters) from the wind turbine and spaced  $45^\circ$  apart. For a given test run, the tower most nearly upwind of the wind turbine was selected as the reference wind station. Both windspeed and wind direction were measured at this point. Atmospheric temperature and barometric pressure data were taken from instruments located in the control room.

### Rain Measurements

During performance tests the occurrence of rain was logged in the test record for the day by the Mod-0 operator. The intensity levels of the rain for rotor configurations I and II were qualitative as perceived by the operator and associated with a period of time, usually several minutes or more. It should be kept in mind that the rain intensity associated for each period of time is an estimated representative value because the actual intensity varied over a single period of time. For performance tests on rotor configuration III, rain intensity levels were recorded automatically by a rainfall measuring device and entered in the Mod-0 database.

Rainfall intensity, for this report, was defined in terms of rates, or mm/hr of precipitation. The following table defines three levels of rain intensity.

Rain intensity levels	Precipitation rate, mm/hr
Light rain	<20
Moderate rain	20 to 30
Heavy rain	>30

### DATA PROCESSING

For this report, evaluation of the effects of precipitation was limited to effects on wind turbine performance, that is, power as a function of windspeed. The analysis was based on the averages of power and windspeed over 2.5 min intervals. This method of analysis was used for several reasons. One reason was that the average performance over a given time period represented the energy captured at various windspeeds. Also, time-averaged data minimized the effects of distance between the meteorological measuring station and the wind turbine. Finally, correction factors for the adjustment of measured alternator power to the rotor were easily applied to time-averaged data.

For the data presented in this report, the wind turbine power output was adjusted as follows: alternator power was converted to rotor power as defined by the appropriate drive-train model, and then corrected to sea-level standard conditions.

### Drive Train Loss Correction

Since alternator power was recorded and rotor power was needed to define aerodynamic performance, drive-train models were derived from calibration tests to define the relationship between rotor power and alternator power. Each drive-train/generator assembly consisted of a low-speed shaft, helical speed increaser, high-speed shaft, V-belt system, and two-speed induction generator. The different drive-train models were required because each configuration had different drive-train system components or operating speeds. Models are shown as follows for each drive-train configuration:

Drive train for configuration I.

$$P_1 = 1.19 P_3 + 10.2 \quad (1)$$

Drive train for configuration II.

$$P_1 = 1.168 P_3 + 7.1 \quad (2)$$

Drive train for configuration III.

$$P_1 = (0.00101 P_3 + 1.094) P_3 + 8.7 \quad (3)$$

where

$P_1$  rotor power, kW

$P_3$  alternator power, kW

#### Density Correction

In order to adjust rotor power to sea-level standard conditions, the local atmospheric pressure and temperature were recorded for each test run. A single correction factor was sufficient for each test run, usually 4 hr in length, because the atmospheric conditions changed very little during this short period of time. Thus, rotor power was adjusted to sea-level standard conditions as indicated by the following equation:

$$P'_1 = \frac{P_1 T_L r_0}{T_0 p_L} \quad (4)$$

where

$P_1$  rotor power, kW

$P'_1$  rotor power adjusted to sea-level standard conditions, kW

$T_L$  air temperature during test, K

$T_0$  air temperature at sea-level standard conditions, K

$p_L$  local air pressure during test, mm Hg

$p_0$  air pressure at sea-level standard conditions, mm Hg

#### EXPERIMENTAL RESULTS

Results of the effects of precipitation on wind turbine performance are presented in the following section in terms of rotor power as a function of windspeed for three rotors operating in various precipitation conditions. The performance data for the three rotor configurations are shown graphically in



figures 5 to 7 . The scatter in the data can be attributed to the fact that the periods and intensities of rainfall were based on qualitative observations and that possible variations in rainfall rates ranged from no rain to extreme rain within a period. Despite the variation in rainfall intensity, the period was specified as having a representative and constant rainfall rate.

#### Configuration I

Rotor performance measured in terms of power as a function of windspeed for configuration I is shown in figure 5. The figure compares data recorded during dry weather conditions with data recorded during light to moderate rainfall conditions and represents ~3 hr of dry conditions and ~3 hr of rainy conditions. The degradation in rotor performance is quite evident at windspeeds above 6 m/s, where most of the data occurred. Neglecting flow retardation, 6 m/s corresponds to an angle of attack of  $9^\circ$  at the 75-percent span station for this rotor. There appeared to be less of an effect when the windspeed was less than 6 m/s. The data shows that moderate rainfall degraded performance by as much as 25 percent in the windspeed range shown.

#### Configuration II

Rotor performance measured in terms of power as a function of windspeed for rotor configuration II is shown in figure 6. The figure compares data recorded during dry conditions with data recorded during light and heavy rainfall and snow-drizzle conditions and represents ~10 hr of dry conditions and ~6 hr of rainy conditions. The degradation in rotor performance as a result of rain is quite evident at windspeeds above 6 m/s, where most of the data occurred. Neglecting flow retardation, 6 m/s corresponds to an angle of attack of  $11^\circ$  at the 75-percent span station for this rotor. From the data it can be seen that light rain degraded performance by as much as 18 percent with high winds, while heavy rain degraded performance by as much as 27 percent. At low windspeeds, snow and drizzle conditions degraded performance by as much as 33 percent.

#### Configuration III

Rotor performance measured in terms of power as a function of windspeed for configuration III is shown in figure 7. This figure compares data recorded during dry conditions to data recorded during rainfall at an average intensity level of 28 mm/hr and represents ~18 hr of dry conditions and ~0.7 hr of rainy conditions. As noted with configuration II, 6 m/s appears to be the windspeed where rain effects become noticeable. Neglecting retardation, 6 m/s corresponds to an angle of attack of  $10^\circ$  at the 75-percent span station for this rotor. The data shows that rain of the indicated intensity level degraded performance by up to 24 percent at higher windspeeds.

Several points can be concluded from the experimental data presented. First, rain degrades the wind turbine performance when the NACA 23024 and NACA 64 series airfoils are used. Second, the heavier the rainfall, the more the degradation in performance. Third, the effects of precipitation become more pronounced as the windspeed increases, corresponding to increasing angles of attack for the blade sections.

## PREDICTION OF RAIN EFFECTS

An analysis was performed to predict the effects of rain on wind turbine performance. This was done in order to correlate and interpret the test data and apply the results to other rotors. Configuration II was selected as the rotor model. A conventional rotor performance code based on blade-element/momentum theory (ref. 4) was used to predict the rotor power as a function of windspeed values. The effects of rain were reflected in the airfoil lift coefficient ( $C_L$ ) and drag coefficient ( $C_D$ ) used by the code.

The use of a method to quantify the effects of rain on airfoil  $C_L$  and  $C_D$  values and the determination of whether that method could be used in wind turbine performance predictions were two critical items evaluated in conjunction with the data analysis. The method for determining the effects on airfoil  $C_L$  and  $C_D$  values was derived from reports published by P. Haines and J. Luers (refs. 1 to 3). In these reports Haines and Luers evaluated, at various rainfall rates, the roughness caused by raindrop cratering on a thin water film and the effect of water-film waviness on airfoils. They equated this roughness to an equivalent sand grain height ( $K_s$ ). With the  $K_s$  value nondimensionalized by division by the chord length  $L$  ( $K_s/L$ ), they then used data from earlier research on airfoil roughness to quantify the roughness (refs. 3, 5, and 6) and to determine the associated aerodynamic penalties.

The  $C_L$  and  $C_D$  as a function of  $\alpha$  curves which reflect the aerodynamic penalties caused by rain are shown schematically in figure 8. The aerodynamic penalties as a result of rain were quantified by four characteristics: (1) reduction in the  $C_L$  at low angles of attack, (2) reduction in the maximum lift coefficient ( $C_{L,max}$ ), (3) reduction in the stall angle ( $\alpha_{stall}$ ), and (4) an increase in the drag coefficient ( $C_{D,o}$ ) at a  $0^\circ$  angle of attack. The procedures for manually constructing the  $C_L$  and  $C_D$  as a function of  $\alpha$  curves are detailed in reference 3.

The curves of  $K_s$  as a function of rainfall rates for both water-drop cratering and water-film waviness at conditions and dimensions typical for large wind turbines are plotted in figure 9. This figure was derived from data in reference 7 and required interpolation from a rainfall rate of 50 to 0 mm/hr to obtain values in the rainfall regime in which the wind turbine operated.

The aerodynamic penalties described in the preceding sections were obtained from references 3, 5, and 6 and are plotted in figures 10 to 13. The lift coefficient values are presented as ratios of the lift, and the change in stall angle and drag coefficient are presented directly. Though these curves were based on results from tests using a NACA 64 series airfoil, it was assumed for this report that they would also apply to the NACA 23024 airfoil used in configuration II.

Airfoil aerodynamic characteristics as affected by rain were determined by applying the adjustments mentioned in the previous section to a baseline airfoil aerodynamic-characteristic data set. This method is described in detail in the following section. The critical parameter,  $K_s$ , was determined from figure 9. The  $K_s$  value used in determining the aerodynamic penalties was the larger of the  $K_s$  values at the appropriate rainfall rate for either the raindrop cratering or water-film waviness. Using appropriate  $K_s$  values for

rainfall rates of 25, 50, and 100 mm/hr and a chord length ( $L$ ) of 1.0 m,  $K_s/L$  values of  $4.0 \times 10^{-5}$ ,  $6.0 \times 10^{-5}$ , and  $1.3 \times 10^{-4}$  were obtained for the three rainfall rates. With these values and information in figures 10 to 13, the aerodynamic penalties of  $\Delta C_L$ ,  $\Delta C_{L,max}$ ,  $\Delta \alpha_{stall}$ , and  $\Delta C_{D,0}$  were determined. In curves for a single element airfoil (figs. 10, 11, and 13) and an airfoil with a 20-percent flap at a  $20^\circ$  deflection, linear interpolation was performed to obtain data at an  $8^\circ$  deflection. Curves of  $C_L$  and  $C_D$  as a function of  $\alpha$  were then constructed to reflect the effects of rain.

The  $C_L$  and  $C_D$  as a function of  $\alpha$  curves used in the blade-element/momentum code were generated with a curve-fitting program. This program adjusted constants that defined the basic airfoil data by the appropriate aerodynamic penalties and empirically modified the poststall data to obtain constant rotor torque after stall (ref. 8).

Because the rotor blade was composed of two sections (single-element airfoil and an airfoil with a deflected 20-percent aileron), two baseline curves were required. The baseline  $C_L$  and  $C_D$  as a function of  $\alpha$  curves were derived from wind tunnel data collected at Wichita State University. The aerodynamic penalties associated with the rain were then applied to these baseline curves. The results of the rain effects on the  $C_L$  and  $C_D$  as a function of  $\alpha$  curves are shown in figures 14 and 15 for the two baseline airfoils at rainfall rates of 0, 25, 50, and 100 mm/hr.

Using the appropriate  $C_L$  and  $C_D$  as a function of  $\alpha$  curves, wind turbine performance, measured in terms of rotor power as a function of wind speed, was predicted for the various weather conditions. The results of these predictions are shown in figure 16. These predictions indicate that rain can have a significant effect on wind turbine performance, even at light rainfall rates. The effects include both a reduction in power, with the highest percentage reduction near maximum power, and a decrease in the windspeed where maximum power occurs. The baseline conditions achieved a maximum power output of 133 kW at a 13.4 m/s windspeed.

A rainfall rate of 25 mm/hr reduced the maximum power to 92 kW at a 12.5 m/s windspeed. This is a 31-percent reduction of maximum power at a 7-percent lower windspeed than that of the baseline curve. A rainfall of 50 mm/hr reduced the maximum power to 81 kW at an 11.6 m/s windspeed. This is a 38-percent reduction in maximum power at a 13-percent lower windspeed than that of the baseline condition. Finally, a rainfall rate of 100 mm/hr reduced the maximum power to 65 kW at a 10.7 m/s windspeed. This is a 51-percent reduction in maximum power at a 20-percent lower windspeed than that of the baseline condition.

Figure 16 also shows the experimental data along with the predicted data. The experimental data for rainfall rates estimated to be in the 20 to 30 mm/hr range indicate a decrease of 18 percent to 27 percent of maximum power at a windspeed of 10 m/s. These percentages are in the range of 25 percent predicted for a rainfall rate of 25 mm/hr at a windspeed of 10 m/s.

## CONCLUDING REMARKS

The Mod-0 wind turbine was operated in dry weather conditions and during periods of precipitation. The effects of precipitation on rotor performance were measured for three different rotor configurations. The three rotor configurations differed in airfoil shape, Reynolds number, and surface roughness; yet all clearly show rotor performance degradation during precipitation. From the measured performance data, it appears that the effects of precipitation seem to become more pronounced as the windspeed and corresponding angle of attack increase. The data also shows that even a light rainfall can measurably degrade rotor performance. For one particular rotor configuration, rotor performance was degraded ~18 percent of the baseline level at rainfall rates of 20 mm/hr or less and ~27 percent of the baseline level at rainfall rates of 30 mm/hr or greater.

An analysis was performed to predict the effects of precipitation on wind turbine rotor power for the 20-percent chord aileron-controlled rotor configuration. A performance prediction code based on blade-element/momentum theory was used. Inherent in the analysis was the evaluation of a method developed by the University of Dayton Research Institute to modify the airfoil lift and drag coefficients reflecting the roughness effects of rain on the airfoil surface and its application to wind turbines. The prediction shows that the effects of precipitation increase with increasing windspeed and that peak rotor power was reduced by 31 percent in a rainfall of 25 mm/hr, 38 percent in a rainfall of 50 mm/hr, and 51 percent in a rainfall of 100 mm/hr. The predicted rotor performance values and trends agreed with the experimental data. Because of the agreement of experimental and predicted data, it appears that the method for adjusting the airfoil lift and drag coefficients to account for rain effects can be applied to wind turbine rotor aerodynamic characteristic modeling.

## REFERENCES

1. Haines, P.A.; and Luers, J.K.: Aerodynamic Penalties of Heavy Rain on a Landing Aircraft. (UDR-TR-82-26, Dayton Univ.; NASA Grant NSG-6026.) NASA CR-156885, 1982.
2. Haines, P.A.; and Luers, J.K.: Aerodynamic Penalties of Heavy Rain on Landing Airplanes. Journal of Aircraft, vol. 20, no. 2, Feb. 1983, pp. 111-119.
3. Haines, P. A.; and Luers, J. K.: Heavy Rain Penalties for a Flight Simulator. AIAA Paper 82-0213, Jan. 1982.
4. Snyder, Melvin H.; and Staples, David L.: Wind-11, Users Manual. WER-15, Wind Energy Laboratory, Wichita State University, July 1982.
5. Brumby, Ralph E.: Wing Surface Roughness Cause and Effect. DC Flight Approach, McDonnell Douglas Corp., no. 32, 1979, pp. 2-7.
6. Ljungstroem, B.L.G.: Wind Tunnel Investigation of Simulated Hoar Frost on a Two-Dimensional Wing Section With and Without High Lift Devices. FFA-AU-902, Aeronautical Research Institute of Sweden, Stockholm, 1972.

7. Luers, J.K.; and Haines, P.A.: The Effect of Rain on General Aviation Aircraft. AIAA Paper 81-1647, Aug. 1981.
8. Viterna, L.A.; and Corrigan, R.D.: Fixed Pitch Rotor Performance of Large Horizontal Axis Wind Turbines. Large Horizontal Axis Wind Turbines, NASA CP-2230, R.W. Thresher, ed., 1982, pp. 69-85. (Also CONF-810752 and SERI/CP-635-1273.)

ORIGINAL PAGE  
OF POOR QUALITY

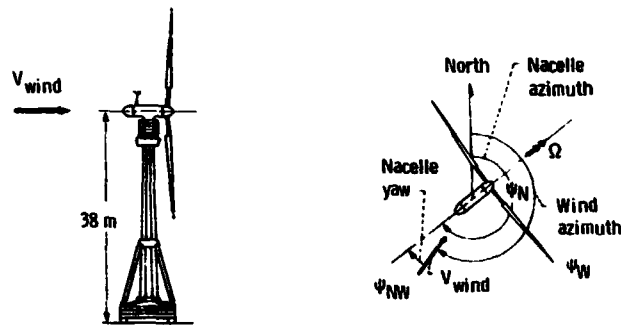
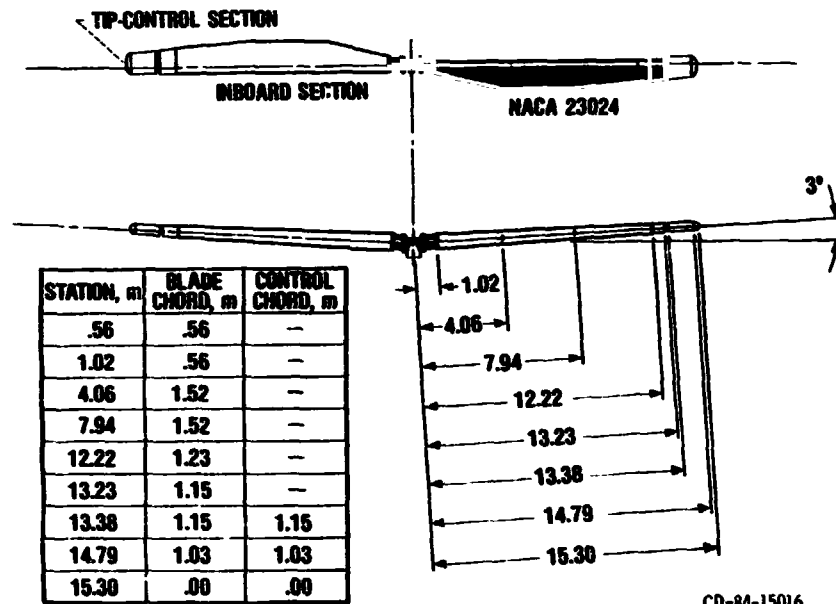


Figure 1. - Schematic of Mod-0 wind turbine located at NASA Plum Brook Station, Sandusky, Ohio.



CD-84-15016

Figure 2. - Tip-controlled rotor planform (configuration I).

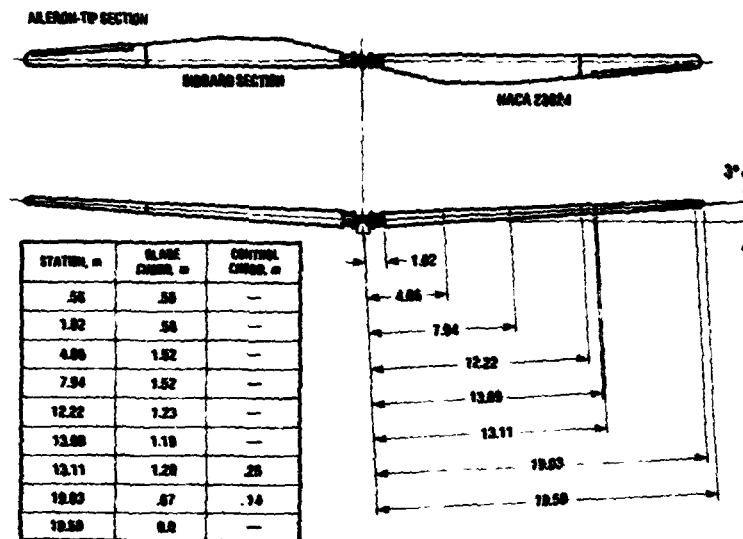


Figure 3. - Planform of 20-percent chord aileron-controlled rotor (configuration II).

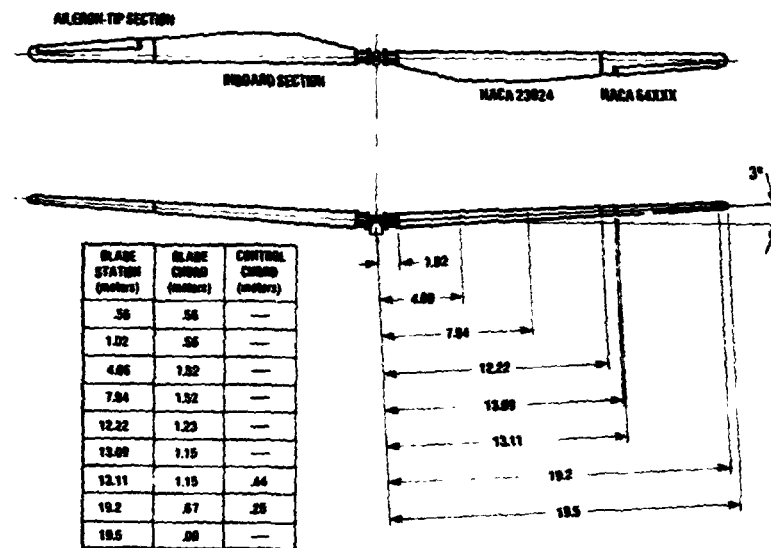


Figure 4. - Planform of 38-percent chord aileron-controlled rotor (configuration III).

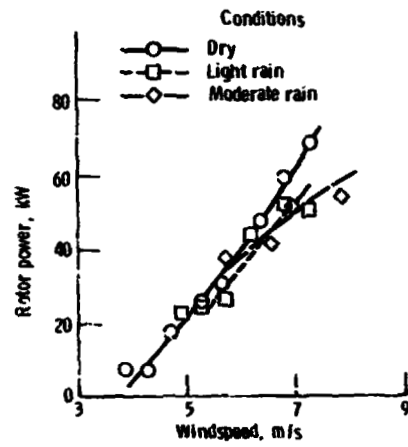


Figure 5. - Rotor performance for configuration I.

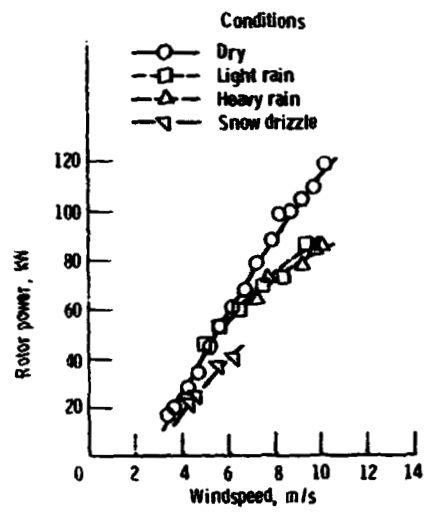


Figure 6. - Rotor performance for configuration II.



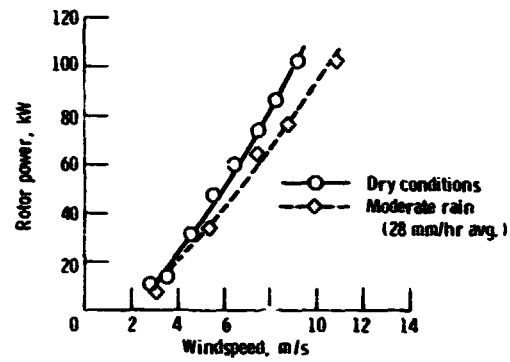
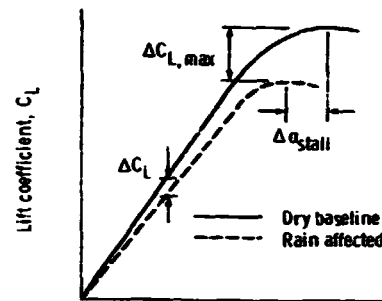
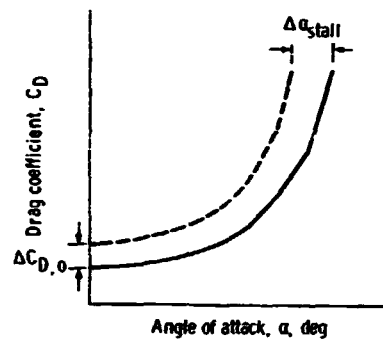


Figure 7. - Rotor performance for configuration III.



(a) Lift coefficient as function of angle of attack.



(b) Drag coefficient as function of angle of attack.

Figure 8. - Penalties on airfoil characteristics as a result of precipitation.

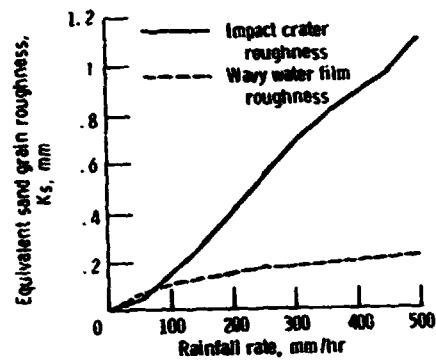


Figure 9. - Equivalent sand grain roughness for various rainfall rates (ref. 7).

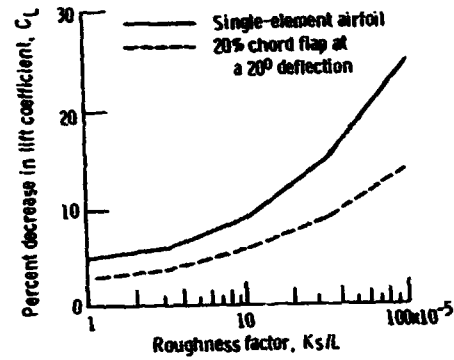


Figure 10. - Decrease in lift coefficient at low angles of attack for various roughness factors (ref. 6).

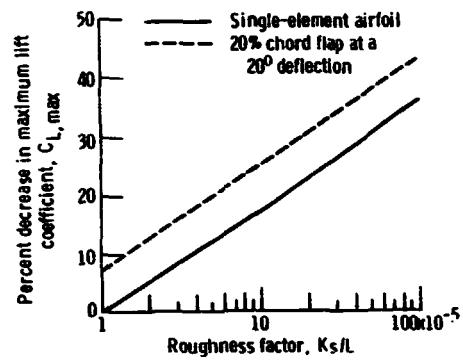


Figure 11. - Decrease in maximum lift coefficient for various roughness factors (ref. 3).

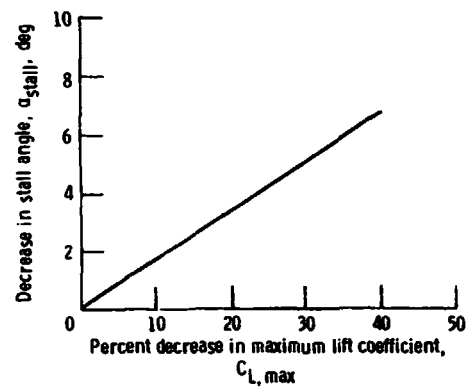


Figure 12. - Decrease in stall angle as function of decrease in maximum lift coefficient (ref. 3).

ORIGINAL PAGE IS  
OF POOR QUALITY

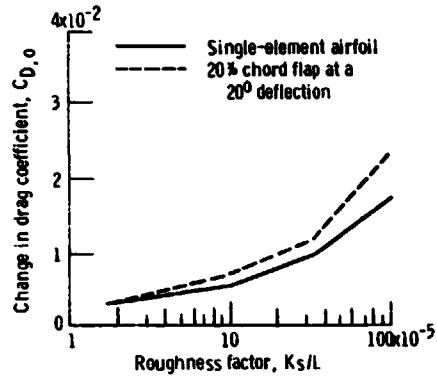
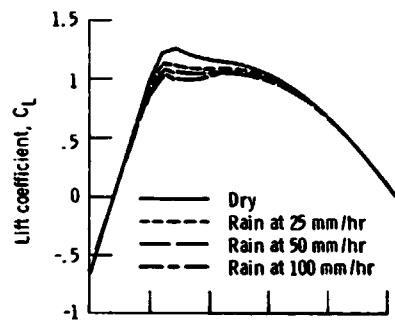
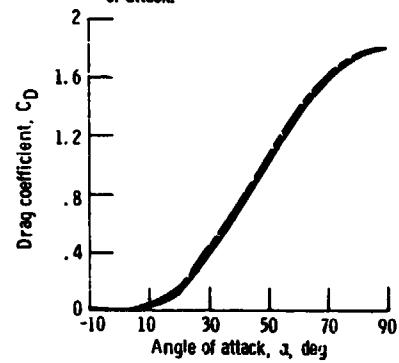


Figure 13. - Change in drag coefficient at  $0^\circ$  angle of attack for various roughness factors (ref. 6).



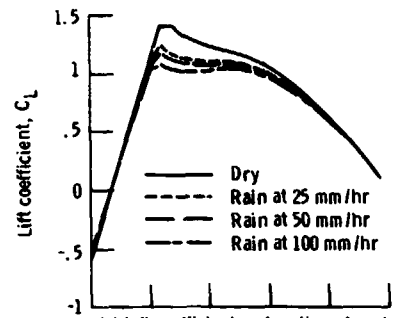
(a) Lift coefficient as function of angle of attack.



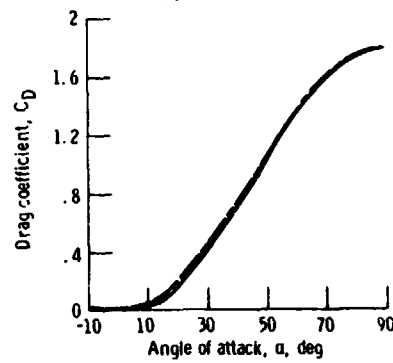
(b) Drag coefficient as function of angle of attack.

Figure 14. - Aerodynamic coefficients for a NACA 23024 airfoil for various rainfall rates.

ORIGINAL PAGE IS  
OF POOR QUALITY



(a) Lift coefficient as function of angle of attack.



(b) Drag coefficient as function of angle of attack.

Figure 15. - Aerodynamic coefficients for a NACA 23024 airfoil with an aileron deflected +8° for various rainfall rates.

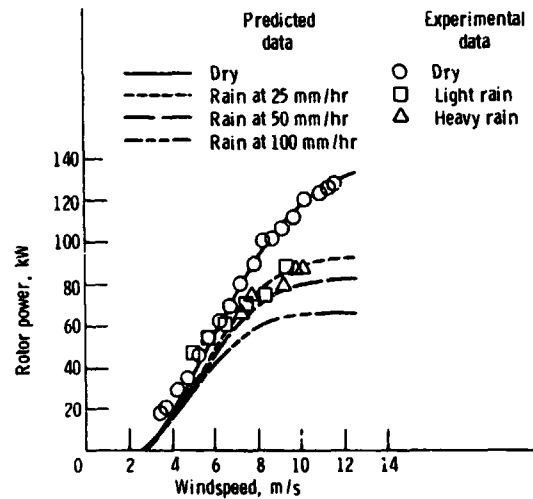


Figure 16. - Comparison between predicted and experimental rotor performance of configuration II for various rainfall rates.

1. Report No. NASA TM-86986		2. Government Accession No.		3. Recipient's Catalog No.	
4. Title and Subtitle  Effect of Precipitation on Wind Turbine Performance				5. Report Date May 1985	
				6. Performing Organization Code 776-33-41	
7. Author(s)  Robert D. Corrigan, Lewis Research Center, and Richard D. DeMiglio, Sverdrup, Inc.				8. Performing Organization Report No. E-2530	
				10. Work Unit No.	
9. Performing Organization Name and Address  National Aeronautics and Space Administration Lewis Research Center Cleveland, Ohio 44135				11. Contract or Grant No.	
				13. Type of Report and Period Covered Technical Memorandum	
12. Sponsoring Agency Name and Address  U.S. Department of Energy Wind Energy Technology Division Washington, D.C. 20545				14. Sponsoring Agency Code Report No. DOE/NASA/20320-64	
15. Supplementary Notes Final report. Prepared under Interagency Agreement DE-AI01-76ET20320.					
16. Abstract  During performance testing on the NASA/DOE Mod-0 100 kW wind turbine, a decrease in rotor power was noted during adverse weather conditions (rain, snow, etc.). A review of the test results indicated this decrease could be attributed to the effects of precipitation on the rotor. Because the decrease in performance was significant, additional tests were run to measure and compare the rotor power with and without precipitation. The test data was analyzed to quantify the effects of precipitation on wind turbine power output. The tests were conducted on the two-bladed Mod-0 horizontal-axis wind turbine with three different rotor configurations. Experimental data from these tests are presented which clearly indicate that the performance of the Mod-0 wind turbine is affected by rain. Light rainfall degraded performance by as much as 20 percent while heavy rainfall degraded performance by as much as 30 percent. Snow mixed with drizzle degraded performance by as much as 36 percent at low windspeeds. Also presented are the results of an analysis to predict the effect of rain on wind turbine performance. This analysis used a blade-element/momentum code with modified airfoil characteristics to account for the effect of rain and predicted a loss in performance of 31 percent in high winds with moderate rainfall rates. These predicted results agreed well with experimental data.					
17. Key Words (Suggested by Author(s))  Wind turbine performance Precipitation effects on performance				18. Distribution Statement  Unclassified - unlimited STAR Category 44 DOE Category UC-60	
19. Security Classif. (of this report) Unclassified		20. Security Classif. (of this page) Unclassified		22. Price* A02	